J Mater Sci (2011) 46:7567–7572
DOI 10.1007/s10853-011-5731-1

Magnetic properties of $Fe_{78.4}Si_{9.5}B_9Cu_{0.6}Nb_{2.5}$ nanocrystalline alloy powder cores

J. Zhou · Y. F. Cui · H. S. Liu · W. Wang · K. Peng · Y. D. Xiao

Received: 6 April 2011 / Accepted: 20 June 2011 / Published online: 28 June 2011

Abstract The microstructure and morphology of nanocrystalline $Fe_{78.4}Si_{9.5}B_9Cu_{0.6}Nb_{2.5}$ alloy powders prepared by ball milling technique were characterized by X-ray diffraction and scanning electron microscopy studies. The effective permeability (μ_e), quality factor (Q), DC bias property, and core losses of the corresponding powder cores were tested using low capacitance resonator meter and B–H analyzer in the range of 1–1000 kHz. The results show that the relative density and compression strength of the powder cores increased with increasing particle size. Powder cores from large size particles (150–300 μm) were found to exhibit higher μ_e and core loss, but lower Q level when compared to samples of small size ones (5–40 μm). Moreover, the μ_e of powder cores with large particles reached a peak value with the addition of 2 wt% glass binder. The Q value was also found to be proportional to the binder content except 10 wt%, while its peak position was shifted toward higher frequency.

J. Zhou · Y. F. Cui · H. S. Liu (✉) · W. Wang · Y. D. Xiao
School of Materials Science and Engineering, Central South University, Mittal Building 222, Changsha 410083, Hunan, People's Republic of China
e-mail: hsliu@mail.csu.edu.cn

K. Peng · Y. D. Xiao
State Key Laboratory of Powder Metallurgy, Central South University, Changsha 410083, Hunan, People's Republic of China

K. Peng
School of Materials Science and Engineering, Hunan University, Changsha 410082, Hunan, People's Republic of China

Introduction

In order to satisfy the demand of industrial electronic devices, soft magnetic cores of nanocrystalline Fe–Si–B alloys have emerged as potential replacements for conventional materials with frequency range of 1–1000 kHz [1], such as ferrites, amorphous ribbons, and metal cores [2–4]. The most widely investigated alloy is $Fe_{73.5}Si_{13.5}B_9Cu_1Nb_3$ (at.%; FINEMET™), which was first reported by Yoshizawa et al. [5]. FINMET is derived from conventional Fe–Si–B system with minor additions of copper (Cu) and niobium (Nb). One of the positive outcomes of amorphous to nanocrystalline transformation is the improvement in soft magnetic properties. Herzer [6] and Hasiak et al. [7] demonstrated that ribbon-type nanocrystalline FINEMET alloys have excellent soft magnetic properties, such as small crystalline anisotropy and nearly zero magnetostriction, due to the formation of nanocrystalline α-Fe(Si) grains dispersed in the residual amorphous matrix [8–11]. Another study by Nowosielski et al. [12] showed that the crystallized ribbons are brittle, which can limit their applications. However, the ribbons were satisfactory for a range of applications such as sensors and pulse generators [13]. For applications requiring good direct current (DC) bias properties and low core losses at high frequency (e.g., large inductors and reactors of power factor correction circuits) [12], ribbons are not suitable. Alternatively, using powder alloys with nanocrystalline structures may be a viable option to overcome these disadvantages. For example, Xu et al. [14] have studied nanostructured powder cores consolidated from flakes (2–15 μm) produced by milling FINEMET ribbons. Their quality factor (Q) of samples in frequency over 50–70 kHz was higher than that made from $Ni_{81}Fe_{17}Mo_2$ (wt%). Cho et al. [15] investigated FINEMET powder cores with the

lowest core loss (59.4 kW/m^3) reached 3 wt% polymer binder after annealing at 600 °C for 1 h. Kim et al. [16] tested cores consolidated from nanocrystalline FINEMET powder (300–850 μm) and 5 wt% of glass binder. They obtained a stable effective permeability (μ_e) of 100 at up to 800 kHz, a maximum level 31 of Q at frequency of 50 kHz, and a core loss of 320 kW/m^3 at $f = 50$ kHz and $B_m = 0.1$ T. Also, Choi et al. [17] reported rotor milled particles (250–850 μm) that showed stable μ_e of 100 at up to 500 kHz, a maximum Q level of 50 at 50 kHz, and 360 kW/m^3 core loss at $f = 50$ kHz and $B_m = 0.1$ T. Müller et al. [18] studied nanocrystalline FINEMET milled powder that was either cold pressed with a mineral binder or hot pressed with a polymer binder (30 vol%). For small particle size (100–160 μm), cold-pressed cores exhibited a flat μ_e of 36 at up to 500 kHz. Increasing the particle size to 250–500 μm promoted μ_e to 80 at 100 kHz. Hot-pressed cores gave μ_e of 65 at 100 kHz. Therefore, it is feasible to combine FINEMET in bulk form via mixing nanocrystalline structure powders with binders, such as mineral as demonstrated by Mazaleyrat and Varga [19] or polymer binder by Ziębowicz [20]. The magnetic properties of the nanocrystalline powder cores can be optimized by adjusting the uniform packing density, particle size, and amount of binder in the cores.

To our knowledge, there is no study of amorphous or nanocrystalline $Fe_{78.4}Si_{9.5}B_9Cu_{0.6}Nb_{2.5}$ (at.%) ribbon. Thus, in this study, we prepared nanocrystalline $Fe_{78.4}Si_{9.5}B_9Cu_{0.6}Nb_{2.5}$ powders by ball milling and investigated the effects of particle size and glass binder (sodium silicate) content on magnetic properties.

Experimental procedures

$Fe_{78.4}Si_{9.5}B_9Cu_{0.6}Nb_{2.5}$ amorphous ribbons with width of 10 mm and thickness about 25 μm were produced by single roller melt spinning technique. Thermal annealing was carried out at 813 K for 40 min in argon atmosphere to obtain nanocrystalline structure. The annealed ribbons were then cut into small pieces of about 100 mm^2, and milled in a planetary ball mill (QM-3SP4 J) with a ball-to-sample weight ratio of 10:1 under argon for 120 min. Powders were sieved into different particle size groups: small (5–40 μm), medium (40–150 μm), and large (150–300 μm). The small and medium size groups were mixed with 2 wt% sodium silicate as the binder, while the large size group was mixed with 1–10 wt% binder. The mixtures were unidimensional consolidated at 1.84×10^3 MPa to produce nanocrystalline powder cores by cold pressing. The heights, inner and outer diameters of the toroidal samples were 10, 19.9, and 33.24 mm, respectively. The samples were annealed at 773 K for 1 h under argon to remove the internal stress and to increase insulation effect.

X-ray diffraction (XRD) spectra of amorphous and nanocrystalline ribbons were collected on a Rigaku D/max-RB diffractometer equipped with a Cu anode. The morphologies of the powder samples were observed via field emission scanning electron microscopy (FESEM) on a FEI Sirion 2000 instrument. The density state of powder cores was measured using the Archimedes method after sealing with wax. The compression strength of toroidal powder cores was examined by mechanical testing on an Instron 3369. The values of μ_e, Q, and the DC bias property of the powder cores were determined by a low capacitance resonator meter (Chroma 3312), while the core losses were measured using a B–H analyzer (Iwatsu SY-8232).

Results and discussion

Figure 1 shows the XRD pattern of $Fe_{78.4}Si_{9.5}B_9Cu_{0.6}Nb_{2.5}$ amorphous ribbons before and after annealing. The wide diffraction peak corresponds to rapidly quenched ribbons occurring within the range of $2\theta = 38°$–$52°$, which is a typical characteristic of amorphous iron alloy (Fig. 1a). In comparison, the annealed samples (Fig. 1b) displayed a sharp diffraction peak at $2\theta = 44.96°$ that represents the (110) plane in addition to (200) and (211) peaks of α-Fe(Si) from crystallized ribbons. The average grain size in the annealed ribbon was determined to be ~15 nm by Scherrer formula [8].

As shown in Fig. 2a, the SEM images showed that the large particles (150–300 μm) were flakes and plates with sharp edges and thickness around 25 μm. Unlike the large size group, the particles from small size group (5–40 μm) have different shapes (Fig. 2c), which were irregular and complex with rounded edges due to agglomeration. The

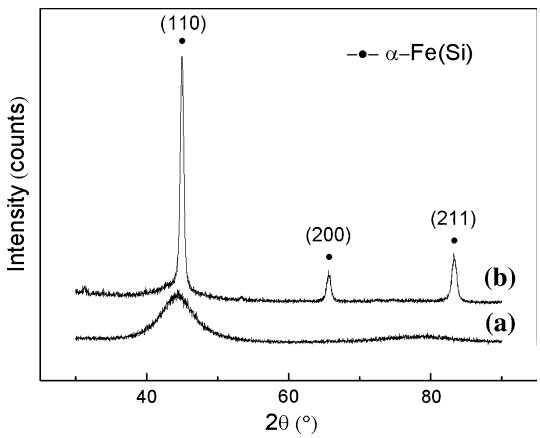

Fig. 1 X-ray diffraction pattern of (*a*) amorphous $Fe_{78.4}Si_{9.5}B_9Cu_{0.6}Nb_{2.5}$ alloy ribbons and (*b*) annealed ribbons

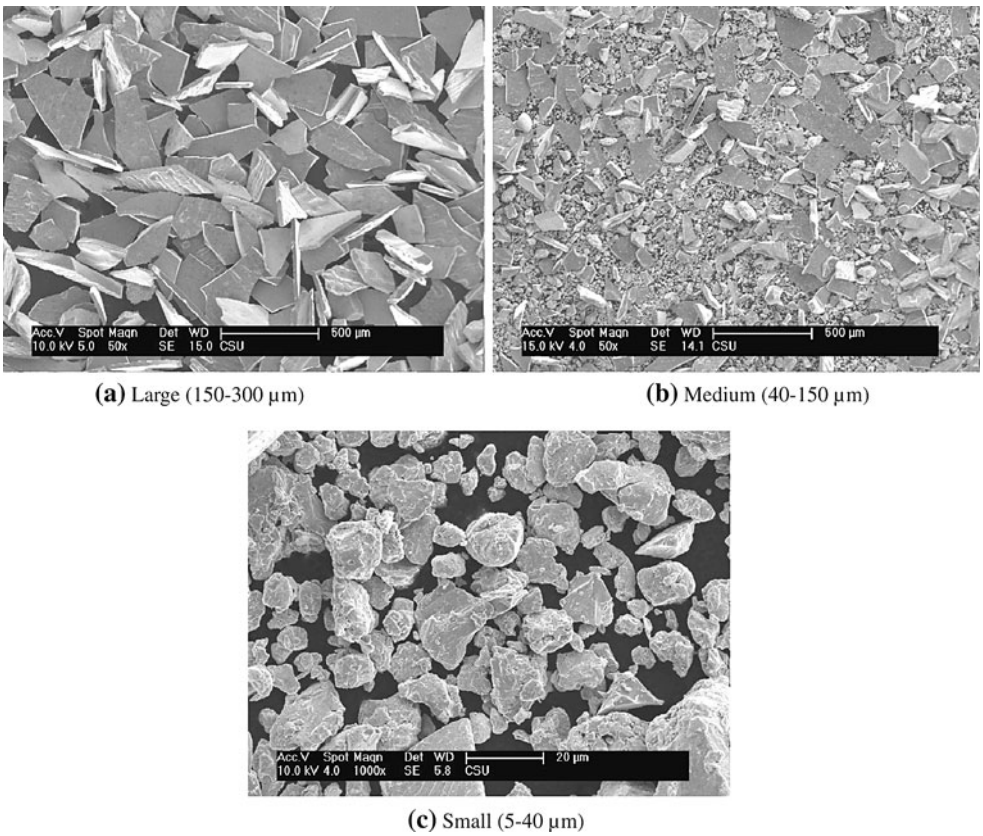

(a) Large (150-300 µm) **(b)** Medium (40-150 µm)

(c) Small (5-40 µm)

Fig. 2 SEM images of powders from each group

medium size samples (40–150 µm) consisted of both large and small particles (Fig. 2b).

The relative density and compression strength of powder cores from different size groups are shown in Table 1. Powder cores made from large size group had the highest relative density, while the density of the small group was 5.43% lower. Moreover, the compression strength of the large group was nearly twice of that of the small group. This is mostly likely due to the fact that larger particles favor the formation of well-aligned microstructure and results in higher density.

The frequency dependence of μ_e and Q for nanocrystalline alloy powder cores of each group with 2 wt% sodium silicate is illustrated in Fig. 3. The results show that within the frequency range tested, the powder cores with larger size particles exhibited higher μ_e, but lower Q. For powder cores made from small particles, a stable level of μ_e at 33 was observed through out the frequency range tested, but a maximum Q level of 86.6 was reached at 100 kHz. For the large and medium size groups, their μ_e values began to decrease slightly at 400 and 600 kHz, while their Q values peaked at 40 and 60 kHz, respectively. The total amount of interface and air-gaps in powder cores made from small particles are much larger than that from

Table 1 Relative density and compression strength of powder cores from each particle size group

Particle range (µm)	Density (%)	σ_{bc} (MPa)
Large (150–300)	82.45	258
Medium (40–150)	79.25	190
Small (5–40)	77.02	135

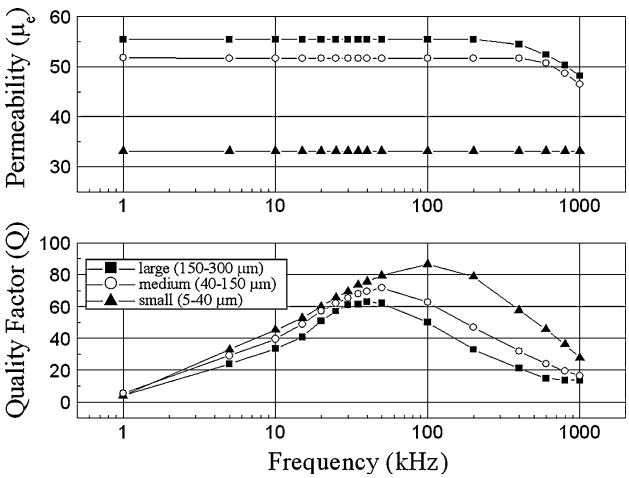

Fig. 3 Frequency dependence of the effective permeability and quality factor for nanocrystalline alloy powder cores made from each group

large ones for irregular shape and huge interaction of small particles made them easy to form bridging. Under an applied magnetic field, the interface and air-gaps of cores would weaken domain wall movement, which would certainly decrease the permeability. In addition, the large demagnetizing stray field due to irregular and complex array of small size powders would also contribute to reduce the μ_e of powder cores made from small group.

Figure 4 presents the frequency dependence of total loss for nanocrystalline alloy powder cores among the different size groups induced at 0.1 T. The core loss was found to increase with increasing particles size under the same experimental condition.

According to the Legg equation [21], the total loss of powder cores in the low frequency can be determined as follows,

$$P = P_e + P_h + P_c \tag{1}$$

where P_e, P_h, and P_c refer to eddy current loss, hysteresis loss, and residual loss, respectively. However, in the medium and high frequency range, P_c could be ignored and the equation can be simplified as:

$$P = P_e + P_h = eB_m^2 f^2 + nB_m^{1.6} f \tag{2}$$

where e and n are the coefficient for P_e and P_c, B_m is the magnetic flux intensity and f is the frequency. It is obvious that the loss of powder cores is mainly related to P_e at medium and high frequency. Based on the cause of the eddy current loss, it could be divided into macroscopic eddy current loss P_e^{ma} and micro eddy current loss P_e^{mi}. Yamauchi and Yoshizawa [22] used a formula to describe this situation:

$$P_e = P_e^{ma} + P_e^{mi} \tag{3}$$

The term P_e^{ma} is the classical eddy current loss and can be determined as follows [22]:

$$P_e^{ma} = \pi^2 d^2 B_m^2 f^2 / 20\rho\eta \tag{4}$$

where B_m is the magnetic flux intensity, d is the particle size, f is the frequency, ρ is the intrinsic resistivity, and η is the core space factor. However, P_e^{ma} is not only related to the intrinsic resistivity and core space factor, but also closely related to the particles sizes and working frequency. For traditional soft magnetic materials such as Fe–Si alloy, P_e^{mi} caused by domain wall displacement is usually significant for very large grain size. However, for the nanocrystalline alloy, the P_e^{mi} is much less than P_e^{ma} and it can be ignored. Therefore, compared to small particles, large particles might cause higher eddy current loss in medium and high frequency range. This may also explain the low core loss of small size group samples.

The DC bias field dependence of nanocrystalline powder cores from each group at 100 kHz, defined by the percentage of μ_e upon DC bias field to μ_e in no DC field, is shown in Fig. 5. The results show that μ_e tends to decrease rapidly for all powder cores from each group when small DC bias current is applied. The percent permeability of cores made from large size samples was 55% at 50 Oe, while that of small size group was 72%. The lower percent μ_e of the powder cores made from larger size group could be attributed to the fact that larger size powders are more easily saturated by low applied magnetic fields. In comparison, powder cores based on conventional soft magnetic alloys such as Sendust [23] and MPP [24] display 40–50% permeability upon 50 Oe of bias field. This indicates that $Fe_{78.4}Si_{9.5}B_9Cu_{0.6}Nb_{2.5}$ nanocrystalline powder cores would yield higher percent permeability when compared to conventional material with the same particle size.

The frequency dependence of μ_e and Q for nanocrystalline powder cores of the large size particles with different contents of sodium silicate is illustrated in Fig. 6. The results show that a maximum value of μ_e was reached

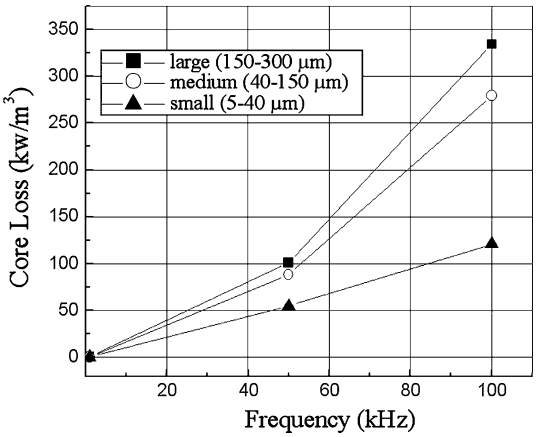

Fig. 4 Frequency dependence of core loss for nanocrystalline alloy powder cores in each group

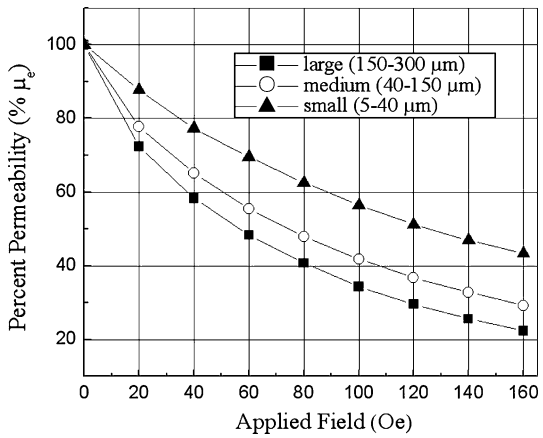

Fig. 5 Plot of the percent μ_e as a function of the DC bias field for nanocrystalline alloy powder cores in each group

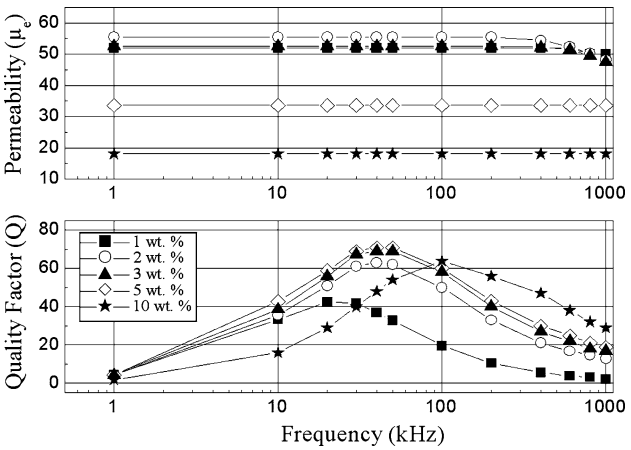

Fig. 6 Frequency dependence of effective permeability and quality factor for powder cores made from large size particles with different contents of glass binder

as the content of sodium silicate was increased to 2 wt%. These samples showed μ_e of 55 at up to 400 kHz and a maximum Q level of 63 at 40 kHz. Within the range of 1–5 wt%, the Q level of powder cores improves and the peaks position of the curves are shifted toward higher frequency with the increase of content. Increasing the binder content improved the insulating effect and reduced the eddy current loss between particles. However, at 10 wt% binder, the corresponding Q value was lower than that of samples with 5 wt% binder. This might be the effect of binder overload. The binder increased not only the insulating effect but also the friction between particles during consolidating process. And the friction might cause more bridging which led to air-gaps. In other words, the powder cores with more binder would be more porous. The increased porosity makes magnetic contents decrease. Therefore, in addition to particle size, binder content also plays an important role in the magnetic properties of nanocrystalline powder cores. Further studies are needed to understand their effects.

Conclusions

Magnetic nanocrystalline alloy powder cores of $Fe_{78.4}Si_{9.5}B_9Cu_{0.6}Nb_{2.5}$ were consolidated with different size particles which were prepared via ball milling process. The grain size of annealed ribbons was determined as $\sim$15 nm. Moreover, the influence of particles size and amount of glass binder (sodium silicate) on magnetic properties were also investigated.

It was found that the physical and mechanical properties of the powder cores were dependent on the particle size and shape. While the powder cores of the large size group (150–300 μm) exhibited the highest relative density of 82.45% and compressive strength of 258 MPa, these properties were at the lowest tested levels (77.02% and 135 MPa) for the cores of the small size group (5–40 μm).

The powder cores made from large group showed stable effective permeability of 55 up to 400 kHz, a maximum Q level of 63 at 40 kHz, and a core loss of 334 kW/m^3 at 100 kHz and 0.1 T. In contrast, with the cores with small particle size group exhibited lower effective permeability of 33 up to 1000 kHz, a higher level of quality factor of 86.6 and a lower core loss of 121 kW/m^3 under same conditions.

In addition, the effective permeability of the large particle powder cores reached a maximum value after the addition of 2 wt% sodium silicate, and the value of Q was found to be proportional to the addition of sodium silicate within 1–5 wt%. However, samples containing high content of sodium silicate (10 wt%) had lower Q value as a consequence of binder overload. The peaks positions of quality factor were shifted toward higher frequency within the range of 1–10 wt%. In general, the particles size and the glass binder (sodium silicate) content were found to significantly affect the magnetic properties of nanocrystalline powder cores.

References

1. Goldman A (1999) Handbook of modern ferromagnetic materials. Kluwer Academic Publishers, Boston
2. McHenry ME, Willard MA, Laughlin DE (1999) Prog Mater Sci 44:291
3. Hilzinger HR (1985) IEEE Trans Magn 21:2020
4. Gungunes H, Yasar E, Dikici M (2011) Int J Min Met Mater 18:192
5. Yoshizawa Y, Oguma S, Yamauchi K (1988) J Appl Phys 64:6044
6. Herzer G (1989) IEEE Trans Magn 25:3327
7. Hasiak M, Ciurzyńska WH, Yamashiro Y (2000) Mater Sci Eng A 293:261
8. Guo M, Wang YG, Miao XF (2011) J Mater Sci 46:1680. doi:10.1007/s10853-010-4985-3
9. Shivaee HA, Golikand AN, Hosseini HRM, Asgari M (2010) J Mater Sci 45:546. doi:10.1007/s10853-009-3972-z
10. Zhu Z, Huang Y, Jiang D, Ma G, Song H (2009) J Wuhan Univ Technol Mater Sci Ed 24:114
11. Fujii H, Yardley VA, Matsuzaki T, Tsurekawa S (2008) J Mater Sci 43:3837. doi:1007/s10853-007-2220-7
12. Nowosielski R, Wysłocki JJ, Wnuk I, Gramatyka P (2006) J Mater Process Technol 175:324
13. Srinivas M, Majumdar B, Akhtar D, Srivastava AP, Srivastava D (2011) J Mater Sci 46:616. doi:10.1007/s10853-010-4770-3
14. Xu H, He KY, Qiu YQ, Wang ZJ, Xiao XS (2000) Mater Sci Eng A 286:197
15. Cho EK, Kwon HT, Cho EM, Song YS, Sohn KY, Park WW (2007) Mater Sci Eng A 449–451:368
16. Kim GH, Noh TH, Choi GB, Kim KY (2003) J Appl Phys 93:7211
17. Choi HY, Ahn SJ, Noh TH (2004) Phys Status Solidi (a) 201: 1879

18. Müller M, Novy A, Brunner M (1999) J Magn Magn Mater 196–197:357
19. Mazaleyrat F, Varga LK (2000) J Magn Magn Mater 215–216:253
20. Ziębowicz B, Szewieczek D, Dobrzański LA (2006) J Mater Process Technol 175:457
21. Legg VE (1936) Bell Syst Tech J 15:39
22. Yamauchi K, Yoshizawa Y (1995) Nanostruct Mater 6:247
23. Magnetics® technical bulletin no. KMS-S1, Kool Mu: a magnetic material for power choke (Butler, 1988)
24. Magnetics® literature MPP-400 6E, molypermalloy powder cores for filter an inductor applications (Butler, 1997)